Available online at www.HighTechJournal.org

HighTech and Innovation Journal

ISSN: 2723-9535

Vol. 7, No. 1, March, 2026

Multi-Dimensional Digital Twin Modeling for Fault Diagnosis of Industrial Centrifugal Pump

Zhengqian Duan [1*]

[1] *School of Mechanical and Electrical Engineering, China University of Mining and Technology, Xuzhou 221116, China.*

Received 11 November 2025; Revised 30 January 2026; Accepted 14 February 2026; Published 01 March 2026

Abstract

Industrial centrifugal pumps operating under complex conditions frequently encounter failures, yet existing diagnostic methods face challenges in effectively fusing multi-source sensor data with physical mechanisms. To address these limitations, this paper proposes a multidimensional digital twin modeling approach that establishes a deep bidirectional synergy between data-driven perception and mechanism-based simulation. First, a Dynamic Sparse Spatio-Temporal Graph Attention Network (DS-STGAT) is designed to capture dynamic local and global dependencies among multi-source signals. Second, unlike conventional unidirectional methods, a novel data-mechanism collaborative adaptive mechanism is introduced. This creates a closed-loop pathway of "data-guided → simulation-refined → data-enhanced," where the perception model retroactively optimizes simulation parameters (e.g., stiffness coefficients) via consistency constraints, while the simulation model provides physical priors to guide graph construction. Experimental results on multiple bearing datasets and real-world pump conditions demonstrate that the proposed method outperforms baseline models in accuracy, physical consistency, and robustness. Notably, the approach achieves high fault identification rates even in zero-shot scenarios, validating its effectiveness and scalability for the intelligent fault diagnosis of complex rotating machinery.

Keywords: Digital Twin Modeling; Multi-Sensor Spatio-Temporal Graph Modeling; Mechanistic Simulation; Industrial Equipment; Fault Diagnosis.

1. Introduction

Industrial centrifugal pumps, as one of the most critical rotating machines in process industries and petrochemical systems, play an irreplaceable role in fluid transportation and energy conversion. They not only undertake core tasks such as long-distance conveyance and process circulation but also directly impact the continuity, safety, and overall energy efficiency of production processes. With the continuous expansion of industrial scale and increasingly complex operating conditions, the operational status of industrial centrifugal pumps has become a key indicator for measuring system stability and reliability. In recent years, rapid advancements in sensor technology, data-driven modeling, and physical simulation methods have enabled multidimensional perception and modeling of centrifugal pump operation. This provides crucial support for achieving intelligent management and digital operation and maintenance throughout the entire equipment lifecycle.

In recent years, fault diagnosis for rotating machinery has evolved from traditional signal processing toward intelligent modeling based on Digital Twins (DT) and Cyber-Physical Systems (CPS). Recent studies have made significant strides in establishing frameworks for these advanced systems. For instance, regarding system architecture, Chakma & Choi [1] integrated 6G technology to construct a real-time digital twin framework, validating its low-latency

* Corresponding author: 03231098@cumt.edu.cn

https://doi.org/10.28991/HIJ-2026-07-01-020

advantages in industrial scenarios. Similarly, Wang et al. [2] systematized the structural design of digital twins by proposing a four-layer conceptual framework, providing a theoretical foundation for equipment health prognosis. Parallel to architectural advances, researchers have focused on the challenge of data scarcity. Lv et al. [3] and Chen et al. [4] explored cyber-physical collaborative strategies, utilizing high-fidelity simulation models to augment training data and addressing feature learning limitations in small-sample scenarios. However, despite these advancements propelling the field, a critical disconnect remains: most existing methods remain predominantly data-driven or unidirectional. While they utilize simulations to generate supplementary data, they fail to establish a deep, bidirectional feedback loop where real-time monitoring data can retroactively refine the physical model's parameters, limiting the system's adaptability and physical consistency under changing operating conditions.

Specifically, multi-source sensor data from rotating machinery exhibits spatiotemporal coupling that dynamically changes with operating conditions, which existing methods struggle to comprehensively model. While mechanism-based models (which rely on first-principles equations to deterministically simulate system dynamics) can explain dynamic behavior, they often remain disconnected from data models, lacking bidirectional feedback. Furthermore, simulation outputs typically yield discrete parameterized results, creating a representational gap with the continuous characteristics of measured signals and hindering direct alignment. These issues lead to insufficient model generalizability under complex operating conditions, as well as diagnostic results lacking stability and physical consistency—defined as the strict alignment of model outputs with fundamental conservation laws and kinematic constraints. This necessitates a modeling approach capable of integrating multi-source perception with mechanism-based simulation.

In the field of multi-sensor spatio-temporal relationship modeling, researchers have proposed various deep learning methods in recent years to capture complex dynamic dependency features during the operation of rotating machinery. Liang et al. [5] proposed a Sample-Rebalanced Spear-Graph Convolutional Network (SRSGCN) for hydraulic axial piston pumps. Their method constructs dynamic graph structures from multi-sensor data to capture inter-sensor correlations, effectively addressing fault diagnosis challenges under limited data conditions. Xia et al. [6] proposed a digital twin-driven local domain fault diagnosis method. This approach generates labeled fault data by constructing a virtual model of rotating machinery and combines it with adversarial transfer learning networks, effectively addressing the scarcity of labeled data in real industrial scenarios. Although these approaches have made progress in multi-source data fusion and spatio-temporal feature extraction, limitations remain. Most methods exhibit insufficient adaptability to dynamic operating conditions and have yet to achieve a balanced integration of multi-scale features—specifically, fine-grained local characteristics versus global system behavior—thereby constraining their generalization capabilities in complex industrial scenarios.

In the field of data-mechanism fusion research, scholars have attempted to introduce physical or simulation models to assist in rotating machinery fault diagnosis, thereby addressing the interpretability and generalization limitations of purely data-driven approaches. Chen et al. [4] conducted a systematic review of intelligent fault diagnosis techniques for rotating machinery under imperfect data conditions. They conducted an in-depth analysis of multi-source data fusion methods, including graph neural networks and attention mechanisms, and constructed a physical experimental platform covering multiple operating conditions and fault types. Xia et al. [6] combined virtual modeling with transfer learning, utilizing labeled virtual fault data to address the scarcity of physical fault data. Their weighted learning module mitigated the negative impact of redundant fault categories, demonstrating the potential for synergistic integration of physical and data models. Li et al. [7] proposed a multi-sensor fusion fault diagnosis method based on adaptive aggregation graph neural networks. They fused acoustic and vibration signals into optimal graph structure data through correlation variance contribution, and employed an improved DiffPool method for feature dimensionality reduction and fault classification, enhancing the model's adaptability under physical information embedding.

Despite these studies achieving positive progress in integrating data with mechanisms, limitations persist at the interactive synergy level. Existing fusion methods predominantly focus on unidirectional information supplementation—such as treating physical models as fixed prior constraints for data models or using simulation data to augment training samples—without establishing a bidirectional closed-loop feedback mechanism between data and mechanisms. For instance, consider a bearing wear scenario: if a physical model only unidirectionally provides simulation data based on initial design parameters (e.g., fixed stiffness), it will fail to reflect the actual stiffness degradation caused by wear. Consequently, this 'prior knowledge' becomes inaccurate as the fault progresses, potentially misleading the data model rather than enhancing it. A critical research gap remains: existing approaches fail to establish a unified framework where data-driven perception and mechanism-based simulation can mutually refine each other dynamically, limiting their accuracy and physical consistency under complex, time-varying conditions.

This paper proposes a multidimensional digital twin modeling framework. Taking industrial centrifugal pumps as the research subject, the framework achieves efficient fault feature extraction through three steps: First, constructing a

dynamic sparse spatiotemporal graph to characterize local and global dependencies among multiple sensors; second, utilizing mechanism model embedding to perform simulation refinement (i.e., the adaptive correction of key physical parameters like stiffness based on data feedback), ensuring model accuracy and reliability under complex operating conditions; Finally, it achieves dynamic alignment and enhancement of simulation and experimental data through closed-loop synergy between data and mechanisms. This approach flexibly captures spatio-temporal dependency features under varying operating conditions, laying the foundation for detailed modeling and experimental analysis in subsequent sections.

The main contributions of this paper include:

- Designing a Dynamic Sparse Spatio-Temporal Graph Approach (DS-STGAT) to capture dynamic correlation features of multi-source sensors across temporal variations and spatial distributions. This approach enables structural self-adaptive adjustment and effective embedding of physical semantic information, thereby enhancing fault feature representation capabilities and diagnostic accuracy.
- Establishing a synergistic adaptive mechanism between data models and physical models. Unlike traditional one-way approaches, this mechanism leverages data-driven features to retroactively optimize key physical parameters—specifically stiffness and damping coefficients—thereby enabling the simulation to dynamically track component degradation (e.g., wear) and achieving deep alignment between the digital twin and the physical system.
- Comparative experiments conducted on actual industrial centrifugal pump operation data and public bearing datasets demonstrate that the proposed method outperforms existing baseline models in accuracy, recall, and robustness metrics. This effectively validates the method's reliability and generalizability under complex operating conditions.

The structure of this paper is as follows: Section 2 introduces related work; Section 3 elaborates on the research framework; Section 4 details the data modeling approach for multi-sensor spatio-temporal graphs; Section 5 presents the bearing mechanism modeling method based on dynamic equations and the reverse knowledge transfer framework; Section 6 demonstrates validation through industrial case studies; finally, Section 7 summarizes the paper and outlines future research directions.

2. Related Works

2.1. Spatiotemporal Feature Extraction from Multi-Sensor Vibration Signals

Vibration signals from rotating machinery contain rich fault information, with different sensors reflecting equipment operating conditions from distinct perspectives. In recent years, researchers have proposed various deep learning methods for spatio-temporal feature extraction. Zheng et al. [8] introduced a flutter detection method integrating signals from internal CNC systems, effectively uncovering dynamic dependencies within time-series data. Li et al. [9] developed a multi-branch parallel perception network designed for multi-sensor feature fusion. Their approach utilizes a hierarchical correlation mechanism to link local sensor features with system-level health status, significantly enhancing fault feature extraction in complex mechanical systems. Although these approaches enhance feature extraction capabilities to some extent, most rely on fixed structures or single time series, making them ill-suited for dynamic dependencies under varying operating conditions. Additionally, they fail to fully integrate multi-scale features at both local and global levels.

2.2. Multi-Sensor Graph Structure Modeling Methods

As the core representation of multi-sensor data, graph structures capture complex dependencies among sensors and serve as a crucial means for multi-view fusion. Li et al. [10] introduced a Wavelet Constrained Physics-Informed Neural Network (WCPINN). By embedding wavelet transform-based physical constraints into the network training process, their method achieves adaptive modeling of fault characteristics while ensuring physical consistency in signal interpretation. Wang et al. [11] developed a traffic demand-based key node identification method for multi-modal transportation networks, which constructs network topology through data-driven approaches to enhance the accuracy of correlation modeling. Xiao et al. [12] proposed a modified multi-scale graph convolutional network combined with 1D-CNNs. Their method dynamically aggregates features from different scales through learnable weights, demonstrating superior capability in capturing complex topological dependencies in rotating machinery data. While these methods exhibit significant advantages in graph representation capabilities, existing research predominantly relies on fixed similarity metrics or predefined topologies. This approach struggles to handle the dynamic nature of data distributions that vary with operational conditions and lacks adaptive strategies for adjusting the importance of features across different views.

2.3. Multi-Scale Feature Extraction in Graph Neural Networks

Multi-scale features capture state patterns at varying granularities, proving particularly crucial for accurately diagnosing continuous degradation faults ranging from minor to severe. Wang et al. [13] designed a similarity metric method for open-set kinship recognition, whose core concept aligns with adaptive multi-scale information selection through cross-layer feature connections. Xu et al. [14] constructed a high-fidelity digital twin system for centrifugal pumps driven by transfer learning. Their framework utilizes graph convolutional neural networks to extract transferrable features across different operating conditions, validating the effectiveness of integrating simulation priors with deep learning for enhanced fault diagnosis. While these methods enhance multi-scale feature representation capabilities, they primarily target static graph structures or system configurations. They lack characterization of dynamic evolutionary processes, and fixed-scale partitioning strategies struggle to adapt to nonlinear failure modes under complex operating conditions.

2.4. Data-Mechanism Integration and Graph-Level Representation Methods

Integrating data with physical mechanisms is a key approach to enhancing diagnostic interpretability and predictive accuracy. Lv et al. [3] proposed a virtual-physical collaborative intelligent fault diagnosis framework for marine rotating machinery under data scarcity, leveraging simulation data to enhance model generalization capabilities in small-sample scenarios. Xia et al. [6] developed a digital twin-driven local domain fault diagnosis method, improving health state prediction accuracy through virtual-physical data alignment. Li et al. [7] proposed a multi-sensor fusion fault diagnosis method for wind turbine bearings based on adaptive aggregation visual graph neural networks, enabling effective knowledge transfer from simulation to data models through physical information embedding. While these approaches demonstrate positive progress in integrating data with mechanisms, most remain limited to unidirectional supplementation: physical models often rely on fixed prior knowledge, lacking the ability to dynamically adjust parameters based on real-time data and lacking data-driven mechanism correction capabilities. Furthermore, they have not established a closed-loop, bidirectional modeling pathway, thereby restricting diagnostic accuracy and adaptability under complex operating conditions.

3. Methodological Framework

Addressing challenges in industrial centrifugal pump fault diagnosis—such as insufficient spatio-temporal correlation modeling of multi-source sensors and the lack of effective coordination mechanisms between data-driven models and physical mechanism models—this paper proposes a multidimensional digital twin modeling framework that integrates multi-source data with physical knowledge, as illustrated in Figure 1. The core of this framework is a bidirectionally synergistic data-mechanism diagnostic architecture: First, a Dynamic Sparse Spatio-Temporal Graph Attention Network (DS-STGAT) is designed. By modeling spatio-temporal dependencies among multi-source sensor data such as vibration and temperature, it enhances the expressive capability of fault features. Second, a data-mechanism collaborative adaptive mechanism is introduced. On one hand, nonlinear dynamics theory is employed to construct a mechanism-based simulation model of the bearing system, guiding and initializing the graph structure of DS-STGAT. On the other hand, a consistency loss function dynamically corrects key parameters in the physical model, establishing a closed-loop path of "data-guided -Simulation Correction-Data Augmentation" closed-loop path. This approach partially resolves the disconnect between data and the physical model, enhancing the model's physical consistency and adaptive capability. Detailed explanations are provided in Chapters 4 and 5.

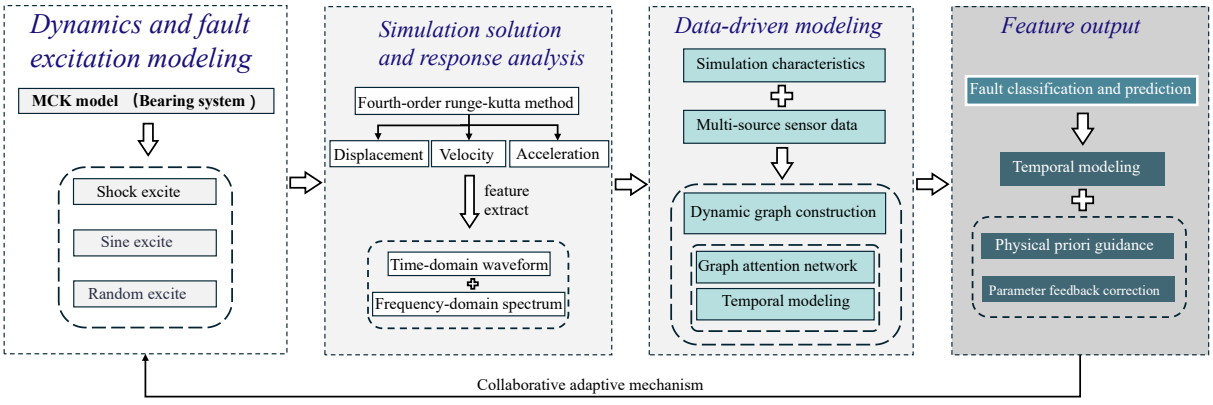

Figure 1. Multi-Dimensional Digital Twin Framework Flowchart

4. Data Modeling Methods for Multi-Sensor Spatio-Temporal Graphs

The proposed Dynamic Sparse Spatio-Temporal Graph Attention Network (DS-STGAT) aims to model spatio-temporal dependencies from both global and local perspectives for multi-sensor data under complex operating conditions of industrial centrifugal pumps. This enables precise extraction and representation learning of critical fault features. To facilitate understanding, the overall pipeline of DS-STGAT is designed as a streamlined 'Graph Construction → Feature Learning → Physics Embedding' process, implemented through four coordinated modules. First, instead of treating sensors as isolated nodes, the Dynamic Graph Structure Construction Module transforms raw data into a graph where edges dynamically evolve to represent changing sensor correlations. Second, the Spatio-Temporal Joint Modeling Module acts as the core engine, using attention mechanisms to learn how fault signals propagate spatially across the equipment and evolve temporally. Crucially, to prevent the model from learning unphysical patterns, the Physical Embedding Module injects simulation data to strictly constrain the learning process. Finally, the Feature Output and Diagnosis Module maps these physically consistent features into interpretable diagnostic results. The detailed structural flowchart is shown in Figure 2.

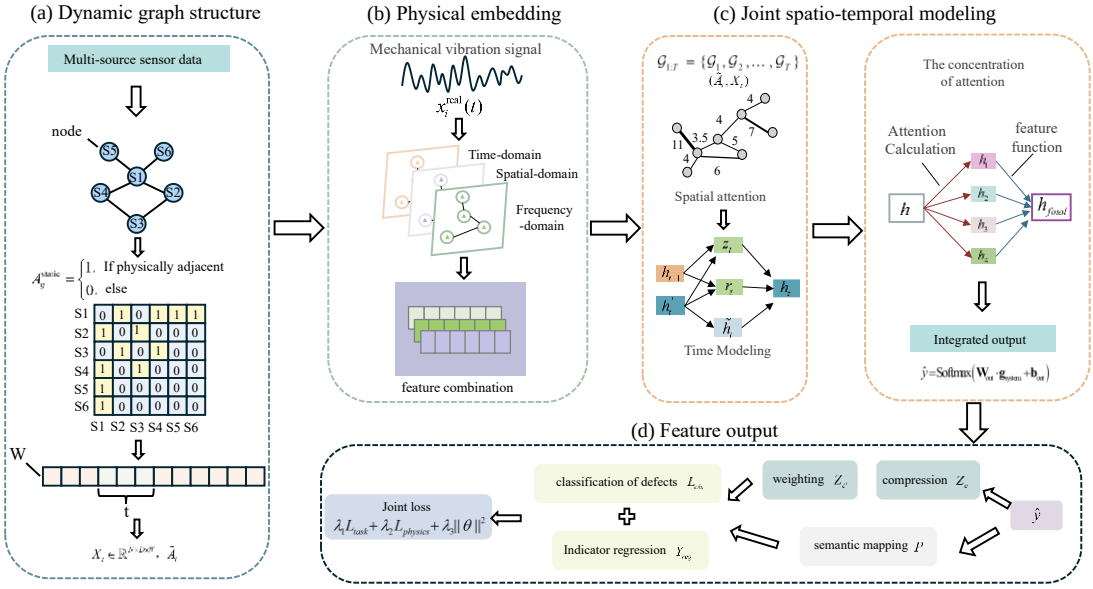

Figure 2. Data Modeling Method Based on Multi-Sensor Spatio-Temporal Graphs

4.1. Dynamic Graph Structure Construction Module

In the condition monitoring and fault diagnosis of bearing systems, data from a single sensor often fails to comprehensively reflect the system's operational characteristics. Particularly in practical engineering applications, minor bearing faults may generate weak response signals only in localized structures. These signals propagate through the system structure to other regions, producing responses with varying amplitudes, phases, and spectral characteristics. Consequently, during bearing fault progression, signals collected from different sensor nodes often exhibit time-evolving spatial coupling relationships and dynamic correlations. To address this, this paper proposes a dynamic graph structure modeling method tailored for bearing systems. This approach abstracts the sensor deployment structure into nodes within a graph structure. By incorporating a sliding window mechanism to dynamically update edge weights between nodes over time, it generates a sequence of graph structures possessing both physical semantics and dynamic characteristics, providing input for subsequent graph neural networks.

First, a static adjacency matrix is constructed based on sensor placement as structural prior knowledge, such as symmetric placement (top/bottom, left/right), axial placement (front/rear), or flange/housing arrangements. This static topology ensures reasonable geometric constraints during model learning. To further characterize the time-varying dynamic dependencies between sensors, this paper calculates the correlation between nodes within a sliding time window. For any two nodes, their correlation within the window is defined by the Pearson correlation coefficient as [15]:

$$\rho_{ij}^{(t)} = \frac{\sum_{k=1}^{D}\sum_{\tau=t-w+1}^{t}\left(x_{i,k}^{(\tau)}-\bar{x}_{i,k}\right)\left(x_{j,k}^{(\tau)}-\bar{x}_{j,k}\right)}{\sqrt{\sum_{k=1}^{D}\sum_{\tau=t-w+1}^{t}\left(x_{i,k}^{(\tau)}-\bar{x}_{i,k}\right)^2}\cdot\sqrt{\sum_{k=1}^{D}\sum_{\tau=t-w+1}^{t}\left(x_{j,k}^{(\tau)}-\bar{x}_{j,k}\right)^2}} \tag{1}$$

Here, $x_{i,k}$ denotes the feature of node i at time k, and $\bar{x}_i$ represents its mean within the window.

Based on the correlation matrix, a threshold θ is set to update the adjacency relations:

$$A_{ij}^{(t)} = \begin{cases} \rho_{ij}^{(t)}, & \omega_{ij}^{(t)} \geq \tau_{\text{corr}} \\ 0, & \omega_{ij}^{(t)} < \tau_{\text{corr}} \end{cases} \tag{2}$$

The resulting dynamic adjacency matrix not only reflects physical dependencies between nodes but also adapts edge weights over time, capturing the propagation characteristics of multi-point responses during fault evolution.

To ensure numerical stability in convolutional operations within graph neural networks, the adjacency matrix is normalized:

$$A_t = D_t^{-1/2} A_t D_t^{-1/2} \tag{3}$$

Here, D_t denotes the corresponding degree matrix. This normalization process prevents highly connected nodes from amplifying effects excessively during feature propagation, ensuring balanced information transfer within the graph structure.

Ultimately, as time progresses, the resulting dynamic graph sequence $\{\mathbf{A}_1, \mathbf{A}_2, \ldots, \mathbf{A}_T\}$ and node feature sequence $\{\mathbf{X}_1, \mathbf{X}_2, \ldots, \mathbf{X}_T\}$ jointly serve as inputs to DS-STGAT, enabling efficient modeling of multi-sensor spatio-temporal dependencies. The empirical superiority of this dynamic topology over static graph structures is quantitatively verified in the ablation study presented in Section 6.3.2 (see Figure 9), particularly in capturing time-varying fault characteristics.

4.2. DS-STGAT Spatio-Temporal Joint Modeling Module

In condition monitoring of multi-sensor bearing systems, sensor node responses exhibit both spatially coupled relationships determined by structural layout and time-dependent characteristics that evolve during operation. Neither static graph modeling nor time-series methods alone can comprehensively capture these cross-dimensional complexities. Static graphs can only reflect fixed topological relationships and cannot dynamically adapt to changes in operational states; traditional recurrent neural networks often neglect heterogeneous spatial dependencies between nodes. To address this issue, this paper proposes a dynamic graph-based spatio-temporal joint modeling framework, DS-STGAT, designed to simultaneously uncover spatial topological patterns and temporal dynamic patterns under a unified structure. This enables high-precision modeling and anomaly detection of bearing system operational states.

This model takes the aforementioned dynamic graph sequence as input, where each time step comprises a node feature matrix and its corresponding dynamic adjacency matrix. Spatial modeling relies on a graph attention mechanism that assigns learnable weights to different adjacency edges beyond traditional adjacency relationships. This highlights the contribution of critical nodes during fault propagation while suppressing interference from noisy or weakly correlated edges. At time step t, the input feature $h_i^{(t)}$ of any node i is calculated using the following formula for its attention score with adjacent node j:

$$e_{ij}^{(t)} = \text{LeakyReLU}\left(\mathbf{a}^T [\mathbf{W}h_i^{(t)} \,\|\, \mathbf{W}h_j^{(t)}]\right) \tag{4}$$

Here, $\mathbf{W}$ denotes the feature mapping weight matrix, $\mathbf{a}$ represents the attention coefficient vector, and $\|$ indicates the feature concatenation operation. This process assigns differentiated weights to distinct adjacency relationships, enabling edge-level importance modeling.

Subsequently, the attention scores undergo SoftMax normalization to yield normalized attention coefficients:

$$\alpha_{ij}^{(t)} = \frac{\exp(e_{ij}^{(t)})}{\sum_{k \in \mathrm{N}_i} \exp(e_{ik}^{(t)})} \tag{5}$$

Then perform the aggregation update by combining all neighboring nodes:

$$\mathbf{h}_i^{(t)} = \sigma\left(\sum_{j \in \mathrm{N}_i} \alpha_{ij}^{(t)} \cdot \mathbf{W}\mathbf{x}_j^{(t)} \right) \tag{6}$$

Here, σ denotes a nonlinear activation function, and N_i represents the adjacency set of node i. Through multi-layer stacking, the model captures multi-order spatial dependencies from local to global scales, enabling local fault information to propagate along the graph structure to the overall state representation.

In the temporal dimension, this paper employs Gated Recurrent Units (GRUs) [16] for sequential modeling of node features, capturing the evolution of states over time. GRUs not only mitigate gradient vanishing but also flexibly adjust

the degree of memory for historical states, making them particularly suitable for progressively accumulating degradation features during bearing operation. Its update expression is:

$$\begin{cases} \mathbf{z}_t &= \sigma\left(\mathbf{W}_z \mathbf{h}_i^{(t)} + \mathbf{U}_z \mathbf{h}_i^{(t-1)}\right) \\ \mathbf{r}_t &= \sigma\left(\mathbf{W}_r \mathbf{h}_i^{(t)} + \mathbf{U}_r \mathbf{h}_i^{(t-1)}\right) \\ \mathbf{h}_t &= \tanh\left(\mathbf{W}_h \mathbf{h}_i^{(t)} + \mathbf{U}_h (\mathbf{r}_t \odot \mathbf{h}_i^{(t-1)})\right) \\ \mathbf{h}_i^{(t)} &= (1-\mathbf{z}_t) \odot \mathbf{h}_i^{(t-1)} + \mathbf{z}_t \odot \mathbf{h}_t \end{cases} \tag{7}$$

Through this temporal modeling approach, the model effectively extracts global evolutionary trends while maintaining short-term sensitivity, forming a continuous description of the fault development process.

During the feature aggregation and output stage, this paper employs global pooling or attention pooling to integrate feature representations from all nodes and time steps into a system-level representation H . This is then fed through a fully connected layer and a SoftMax classifier to output the final health status:

$$\hat{y} = \text{Softmax}\left(\mathbf{W}_o \cdot \mathbf{g}_{\text{system}} + \mathbf{b}_o\right) \tag{8}$$

Here, $\mathbf{W}_o$ and $\mathbf{b}_o$ are learnable parameters. This output enables both real-time health status identification at the current time step and can be further extended to downstream tasks such as fault trend prediction and remaining life assessment. Consequently, DS-STGAT not only achieves spatiotemporal joint modeling of multi-sensor signals but also ensures progressive feature extraction from local fault excitation to global state representation through its structural design, providing an effective pathway for fault diagnosis under complex operating conditions.

4.3. Physics-Embedded Module for Data Model Optimization

This module integrates vibration single-mode data generated by mechanism-based simulation models, guiding graph neural networks to incorporate physical prior knowledge during initialization while introducing physical consistency constraints throughout training. This enables parameter transfer and high-quality feature learning tailored to structural degradation evolution. Compared to purely data-driven approaches, this mechanism not only enhances model generalization under data scarcity or complex operating conditions but also endows the network learning process with explicit physical semantics.

Taking a bearing system as an example, a dynamic simulation model is first run based on an initial set of physical parameters (e.g., mass, stiffness, damping) to obtain vibration response sequences at various sensor points. Although this response constitutes a single-mode vibration signal, it contains rich physical information. Features can be extracted from three complementary dimensions:

- Time-domain features: Describe the overall amplitude level and fluctuation characteristics of the signal by calculating statistical metrics such as mean, root mean square (RMS), peak factor, and kurtosis.
- Frequency-domain features: Utilizing the Fast Fourier Transform (FFT) [17] to extract dominant frequencies, bandwidth, and spectral centroid, reflecting energy concentration across the system's frequency distribution;
- Spatial features: Characterizing the propagation patterns of localized faults to the overall system by comparing modal differences and structural coupling strengths among different sensing points.

Combining these features forms the initial node embedding $\mathbf{H}_0$, serving as input to the graph neural network:

$$\mathbf{H}_0 = f_{\text{embed}}(\mathbf{s}_{time}, \mathbf{s}_{freq}, \mathbf{s}_{space}) \tag{9}$$

Here, $\mathbf{s}_{time}$, $\mathbf{s}_{freq}$, and $\mathbf{s}_{space}$ represent three types of features, respectively, while $f_{\text{embed}}(\square)$ denotes the embedding function. This embedding ensures the complete expression of physical semantics across multiple dimensions of vibration modes, providing a reasonable initialization for subsequent learning processes. For instance, consider a scenario where the simulation predicts a high energy response at the characteristic Ball Pass Frequency Outer race (BPFO) simultaneously at the bearing housing and the pump base. Even if the actual measured signals at these locations are contaminated by background noise, the physical embedding (encoding this simulated spectral correlation) will initialize a strong edge weight between these two sensor nodes. This effectively guides the Graph Attention Network to focus on this physically valid transmission path, preventing the model from being misled by spurious noise correlations.

As equipment operates, physical parameters undergo gradual evolution—such as stiffness reduction due to wear in bearing rolling elements or raceways, or damping changes caused by deteriorating lubrication conditions. To enable the model to adapt to these variations, this paper designs a parameter self-adaptive correction mechanism. This mechanism utilizes the discrepancy between measured vibration responses and simulated responses to perform inverse optimization on parameter Θ :

$$\Theta^{(t+1)} = \Theta^{(t)} - \eta \frac{\partial \mathrm{L}_{phy}}{\partial \Theta^{(t)}}, \tag{10}$$

Here, η denotes the learning rate, and $\mathbf{L}_{phy}$ represents the loss function under physical consistency constraints. Through this update mechanism, parameter evolution aligns with the actual degradation trends of the device, preventing the model from falling into pure data fitting.

To ensure graph neural networks remain grounded in physical mechanisms during feature extraction, this paper incorporates a physical consistency constraint into the training objective. Specifically, the final node representation h_i undergoes a Fourier transform to yield spectral features. These are aligned with the measured signal spectrum, and the consistency error in the frequency domain is computed. This error is then combined with the diagnostic task loss to form the overall objective function:

$$\mathrm{L}_{\text{total}} = \mathrm{L}_{\text{task}} + \lambda \mathrm{L}_{\text{phy}} \tag{11}$$

where, L_{task} represents the fault classification or prediction loss, and λ denotes the trade-off factor. This design enables the model to learn fault-sensitive features while ensuring interpretability in frequency identification and degradation mechanisms.

In summary, the physical embedding module achieves seamless integration of data and mechanisms through a closed-loop path: initialization with simulation data, adaptive parameter refinement, and physical consistency constraints. This module not only fully exploits the multidimensional potential of single-mode vibration data across time, frequency, and spatial domains but also enhances the model's adaptability and interpretability toward fault evolution through dynamic transfer mechanisms, providing robust support for subsequent diagnostic tasks.

4.4. Feature Output and Diagnosis Module

After completing dynamic graph structure modeling and spatio-temporal feature extraction from multi-source sensor data, the DS-STGAT model outputs high-dimensional, multi-semantic feature representations for each sensor node. These features integrate the node's temporal dynamics with its spatial dependencies on other nodes within the graph structure, exhibiting strong discriminative power and physical coupling semantics. However, the feature dimensions output by raw graph neural networks are often excessively high. Direct application to diagnostic tasks poses challenges such as substantial computational overhead, high overfitting risks, and weak engineering interpretability. To address this, this paper designs a diagnostic module incorporating feature compression and selection, physical-semantic mapping, and task-discrimination optimization. This module aims to project deep features onto an engineering-relevant semantic space, thereby enabling health status recognition or fault indicator prediction for industrial equipment.

First, during the feature compression and selection phase, the spatio-temporal feature matrix output by DS-STGAT undergoes dimensionality reduction and filtering. High-dimensional representations may contain redundant or weakly discriminative dimensions, which are compressed into low-dimensional representations via a linear mapping layer:

$$\mathbf{Z} = \mathbf{W}_c \mathbf{H} + \mathbf{b}_c \tag{12}$$

Here, $\mathbf{H}$ represents high-dimensional features, $\mathbf{W}_c$ and $\mathbf{b}_c$ denote mapping parameters, and $\mathbf{Z}$ denotes low-dimensional representations. To further enhance discriminative power, an attention-weighted mechanism can be integrated to adaptively adjust weights across different dimensions, thereby highlighting feature dimensions more strongly correlated with faults.

During the physical semantic mapping phase, this paper introduces a set of learnable mapping weights to project deep features onto an indicator space with engineering-physical significance:

$$\mathbf{F} = \mathbf{W}_p \mathbf{Z} + \mathbf{b}_p \tag{13}$$

The $\mathbf{F}$ denotes that the projected semantic vector $\mathbf{W}_p$ is a learnable parameter. Dimensions in this space can correspond to specific physical metrics, such as vibration impact intensity (correlated with kurtosis), dominant frequency energy ratio (correlated with spectral energy distribution), energy difference between adjacent nodes (reflecting structural transmission anomalies), and graph embedding inconsistency (indirectly revealing local stiffness variations). Through this mapping, the high-dimensional representations obtained by deep learning establish connections with interpretable physical quantities, thereby enhancing the engineering reproducibility and physical interpretability of diagnostic models. Furthermore, physical constraints (such as energy conservation and frequency distribution boundaries) can be introduced at this stage to further improve the reliability of feature representations.

During the task discrimination phase, the model can perform classification or regression based on specific requirements. For typical fault classification tasks, a SoftMax output and cross-entropy loss function are employed:

$$L_{cls} = -\sum_{c=1}^{C} y_c \log(\hat{y}_c) \tag{14}$$

Where, $\hat{y}_c$ represents the predicted probability and y_c denotes the one-hot encoding of the true label. For regression tasks such as fault indicator prediction or remaining life assessment, the mean squared error (MSE) is employed as the loss function.

Considering the end-to-end training requirements of the entire DS-STGAT system, this paper integrates diagnostic loss, physical consistency constraints, and parameter regularization terms into the final optimization objective. The joint loss function is defined as:

$$L = L_{diag} + \lambda_{phy} L_{phy} + \lambda_{reg} \| \Theta \|^2 \tag{15}$$

Here, L_{diag} represents the loss for classification or regression tasks, L_{phy} denotes the loss from the physical consistency constraint module, $\|\Theta\|^2$ is the regularization term, and λ_{phy}, λ_{reg} are trade-off hyperparameters. This joint loss design ensures a global balance among diagnostic accuracy, physical interpretability, and model stability, providing a solid foundation for subsequent system-level closed-loop deployment.

5. Mechanism Modeling Method for Industrial Centrifugal Pumps Based on Kinematic Equations

During the long-term operation of industrial centrifugal pumps, bearings serve as the core components supporting rotor rotation and transmitting loads. Their health status decisively impacts the stability and reliability of the entire machine. Confronted with complex fault excitations, nonlinear coupled behaviors, and dynamically evolving physical parameters commonly encountered in industrial settings, traditional static simulation models struggle to accurately model and interpret actual operating conditions. Therefore, to enhance the physical consistency, interpretability, and dynamic adaptability of digital twin systems, this paper introduces a nonlinear dynamic modeling approach tailored for bearing systems. This approach constructs simulation modules featuring engineering semantics, adjustable structures, and closed-loop collaboration with data models. The mechanism modeling method is illustrated in Figure 3.

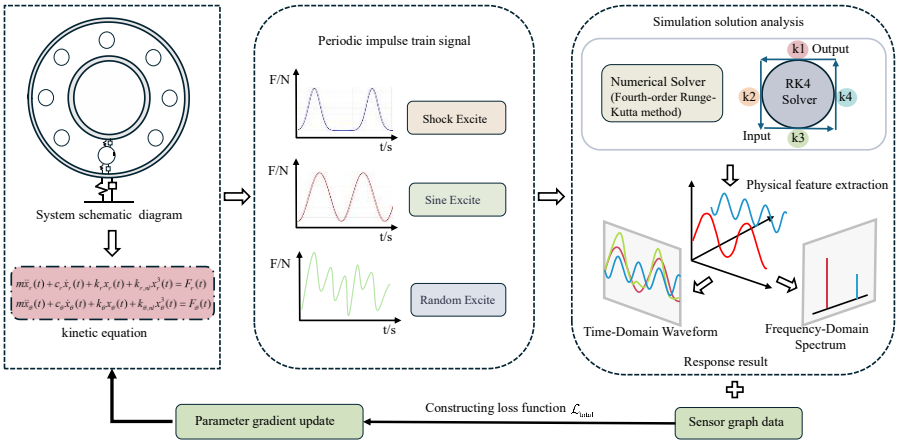

Figure 3. Mechanism Modeling Methods

This section clarifies the core objectives of mechanism modeling and proposes reasonable modeling boundaries and assumptions, providing foundational support for subsequent formula derivation and system implementation across submodules. The overall objectives are summarized in two dimensions:

(1) Response Modeling:

Focusing on the structural vibration response of bearing systems, construct a dynamic model capable of handling multi-source fault excitation inputs, nonlinear structural coupling, and dynamic evolution. Simulate the time-domain and frequency-domain response characteristics of industrial centrifugal pumps under typical fault conditions (e.g., bearing spalling, imbalance, rubbing). This provides the foundation for subsequent physical a priori embedding and structural semantic transfer.

(2) Reverse Constraint:

Key structural response features learned by data models (e.g., DS-STGAT) from measured data are fed back to the mechanism model through feature mapping mechanisms. A consistency loss function is constructed to guide dynamic adjustments of simulation parameters (e.g., stiffness, damping, impact cycles), thereby establishing a closed-loop optimization mechanism between data and simulation.

5.1. Dynamic Modeling Structure of Bearing Systems in Industrial Centrifugal Pumps

As critical support and guidance components in industrial centrifugal pumps, the operational status of bearing systems directly impacts the vibration characteristics and stability of mechanical equipment. Bearings comprise multiple elements including rolling elements, retainers, and inner/outer rings, whose interactions determine the dynamic response characteristics of the bearing. In industrial environments, bearings are prone to failures such as wear, spalling, and cracking, leading to nonlinear changes in stiffness and damping characteristics that compromise the safe operation of the entire equipment. Therefore, this section focuses on the dynamic modeling of the bearing system, emphasizing the dynamic behavior in both radial and angular degrees of freedom. The influence of the rotor system is temporarily disregarded to more accurately reflect the impact patterns of bearing structural failures on dynamic response.

The dynamic characteristics of a bearing system are typically described using the classical mass-damping-stiffness (MDS) model. In this model, the internal rolling elements and cage of the bearing are equivalent to a mass block, elastic deformation is represented by stiffness elements, and energy dissipation processes are embodied by damping elements. System vibrations primarily manifest in radial and angular directions, enabling the establishment of a two-dimensional, two-degree-of-freedom model. Let the equivalent mass be m, the radial and angular damping coefficients be c_r and c_θ, respectively, the linear stiffnesses be k_r and k_θ, respectively, the radial and angular displacements be x_r and x_θ, respectively, and the excitation forces be F_r and F_θ, respectively. The fundamental dynamic relationship of the system can then be expressed as:

$$m\ddot{x}_r + c_r\dot{x}_r + k_r x_r = F_r, \quad m\ddot{x}_\theta + c_\theta\dot{x}_\theta + k_\theta x_\theta = F_\theta \tag{16}$$

Under actual industrial operating conditions, bearing stiffness exhibits pronounced nonlinear characteristics, particularly when defects, wear, or spalling are present, as elastic deformation no longer satisfies the linearity assumption. To simulate stiffness discontinuities caused by localized structural damage, a cubic nonlinear stiffness term can be introduced to modify the linear stiffness:

$$k_r x_r + k_{r,NL} x_r^3, \quad k_\theta x_\theta + k_{\theta,NL} x_\theta^3 \tag{17}$$

Among these, $k_{r,NL}$ and $k_{\theta,NL}$ represent the radial and angular nonlinear stiffness coefficients, respectively, typically positive values reflecting the physical phenomenon where stiffness increases rapidly with displacement. The nonlinear terms effectively capture stiffness discontinuities and jumps caused by local defects, thereby enhancing the sensitivity of fault diagnosis to abnormal dynamic characteristics.

For numerical solution and coupled analysis, the system can be represented in matrix form, though matrix formulas are not listed separately in this version. Specifically: - The state vector comprises radial and angular displacements and velocities. - The mass matrix is diagonal, representing the inertial effects of each degree of freedom. the damping matrix is diagonal or approximately diagonal, reflecting lubricant film friction and material damping; the stiffness matrix incorporates both linear and nonlinear components, with the nonlinear portion dynamically adjusting with displacement; the excitation vector comprises radial and angular external and fault excitations, which may vary with time or operating conditions. The physical interpretations of model parameters are shown in Table 1.

Table 1. The physical meaning of model parameters

Parameter Category	Parameter Symbol	Physical Meaning
Quality	m	The equivalent mass of the rolling elements and cage inside a bearing determines the system's inertial effects
Damping Coefficient	c_r , c_θ	Represents the friction of the lubricating oil film on bearings and the damping properties of the material itself, affecting the rate of vibration decay in the system
Linear stiffness	k_r , k_θ	Reflection of the bearing's elastic deformation capacity
Nonlinear Stiffness	$k_{r,NL}$, $k_{\theta,NL}$	Reflects nonlinear elastic responses caused by defects or wear
Excitation force	$F_r(t)$, $F_\theta(t)$	Intrinsic motivation or external disturbance force during a fault state

5.2. Typical Fault Excitation Modeling Methods

In the process of mechanistic modeling for bearing systems, modeling excitation forces is crucial. As support components for high-speed rotating machinery, bearings possess complex internal structures and are subjected to various types of excitations during operation. These excitations may originate from manufacturing errors, assembly deviations, or inadequate lubrication, or result from periodic or non-steady impacts caused by structural defects such as spalling, cracks, or deformation.

To accurately reflect the dynamic response behavior of bearing systems under different failure modes, this section constructs three typical excitation models based on the physical mechanisms of excitation sources: impact excitation, sinusoidal excitation, and random excitation. Furthermore, a composite modeling framework for multi-source excitation superposition is proposed to enhance the applicability and expressive capability of the models.

In the mechanism-based modeling of bearing systems, modeling excitation forces is critical. As support components for high-speed rotating machinery, bearings possess complex internal structures and experience multiple excitation effects during operation. These include manufacturing errors, assembly deviations, poor lubrication, and periodic or non-steady impacts caused by structural defects such as spalling, cracks, or localized deformation. To accurately reflect dynamic response behavior under different failure modes, this section constructs three typical excitation models—impact, sinusoidal, and random—based on the physical mechanisms of excitation sources. A composite modeling framework incorporating multi-source excitation superposition is proposed to enhance the model's applicability and expressive capability.

Impact excitation primarily corresponds to localized structural damage in bearing raceways or rolling elements, such as inner ring spalling, outer ring pitting, or rolling element notches. Each time a rolling element passes through the defect zone, it generates a short-duration, high-frequency impact that excites an instantaneous system response. This excitation exhibits distinct periodicity and non-stationarity, appearing as a pulse train in the time domain and displaying a characteristic amplitude-modulated sideband structure in the frequency domain. For modeling purposes, it can be approximated using periodic pulse sequences, typically simulated with narrow-pulse-width Gaussian pulses.

$$F_{\text{impact}}(t) = \sum_{n=0}^{\infty} A_{\text{impact}} \exp\left(-\frac{(t - nT_{\text{impact}})^2}{2\sigma^2} \right) \tag{18}$$

Here, A_{impact} denotes the impact amplitude, reflecting the severity of the defect; T_{impact} represents the impact period, determined by the defect location and bearing geometric parameters; σ controls the impact duration. Typical bearing failure frequencies (such as inner ring, outer ring, or rolling element failure frequencies) can be calculated based on the number of rolling elements, diameter, pitch diameter, contact angle, and bearing rotational speed. However, the formulas are presented here in textual form to maintain the overall flow of the chapter.

Sinusoidal excitation primarily originates from unbalanced masses or eccentric loads within the system. Even when the rotor system is not directly modeled in this section, eccentric masses transmit periodic sinusoidal forces through the bearings to the foundation structure. This excitation drives the system's fundamental harmonic response and higher-order components, modeled as:

$$F_{\text{sin}}(t) = A_{\text{sin}} \sin(2\pi f_{\text{rot}} t + \phi) \tag{19}$$

Here, A_{sin} denotes the excitation amplitude, which correlates with the eccentric mass and rotational speed; f_{rot} represents the rotational frequency; ϕ is the initial phase, used to control the excitation phase characteristics. This formula is one of the core formulas retained, while other periodic excitation characteristics can be described verbally, such as amplitude variation with rotational speed and periodic coupling with the system's natural frequency.

Random excitation simulates irregular disturbances encountered by bearings during start-stop cycles or transient operation, such as intermittent impacts, lubrication anomalies, or sudden load changes. Characterized by randomness and non-stationarity, it can be modeled using random processes like white noise or randomly enveloped pulse sequences. White noise describes high-frequency background vibrations, while pulse sequences more closely approximate irregular contact processes between rolling elements and defect zones. Impact amplitudes may follow a specific distribution, and excitation timing can be controlled via a Poisson process. Specific formulas are not provided here; instead, their statistical characteristics are described verbally.

In actual operating conditions, bearing systems typically experience the combined effects of periodic excitation, impact excitation, and random disturbances simultaneously. Therefore, a multi-source composite excitation model must be constructed. This composite model can be achieved through linear weighted superposition:

$$F_{\text{total}}(t) = w_{\text{impact}} F_{\text{impact}}(t) + w_{\text{sin}} F_{\text{sin}}(t) + w_{\text{rand}} F_{\text{rand}}(t) \tag{20}$$

Here, w_{impact}, w_{sin}, and w_{rand} represent weighting coefficients that can be adjusted based on the dominant failure mechanisms under different operating conditions to ensure the model accurately reflects the combined effects of multi-source excitation on the bearing system.

5.3. Simulation Solving and Dynamic Response Analysis

Nonlinear dynamic models of bearing systems typically lack analytical solutions when subjected to typical fault excitation, necessitating dynamic simulation solving through numerical methods. By analyzing the displacement, velocity, acceleration, and spectral responses of the system under various excitation inputs, characteristic patterns induced by different faults can be revealed. This provides embeddable physical response information for subsequent data-driven modeling and supports the interpretability of diagnostic tasks.

The nonlinear dynamic equations of bearing systems typically lack analytical solutions, necessitating the use of numerical integration methods for dynamic simulation and solution. Consider the nonlinear dynamic equations for a two-degree-of-freedom system:

$$M\ddot{x}(t)+C\dot{x}(t)+K(x)x(t)=F(t) \tag{21}$$

Where, $x=[x_r,x_\theta]^T$ represents radial and angular displacement, M, C, and K denote the mass, damping, and nonlinear stiffness matrices respectively, and $F(t)$ is the excitation force.

To facilitate numerical solution, the second-order equation is converted into a first-order differential form. By defining the state vector $X=[\dot{x},\ddot{x}]$, the system's state evolution can be expressed as:

$$\dot{X}=f(X,t) \tag{22}$$

Here, $f(X, t)$ incorporates the effects of damping, nonlinear stiffness, and external excitation.

Based on this, the system is integrated using the fourth-order Runge-Kutta method [18]. The specific procedure is as follows:

During the numerical solution process, the simulation time is divided into multiple time steps, each with a duration of Δt. Within each time step, an intermediate estimate of the state increment is first calculated, and the system state is updated using a weighted averaging method. Subsequently, the system state is iteratively updated throughout the entire simulation time interval to obtain the displacement, velocity, and acceleration responses of the bearing system.

The output responses comprise the following three categories:

- Displacement responses: $x_r(t)$, $x_\theta(t)$;
- Velocity and acceleration responses: obtained through numerical differentiation;
- Frequency domain response: transformed using the Fast Fourier Transform (FFT) [17].

Under different fault excitation conditions, the bearing system exhibits distinctly differentiated response patterns:

Impact Excitation: In the time domain, it manifests as periodic sharp pulses; in the frequency domain, peaks appear at the impact cycle frequency, accompanied by observable amplitude-modulated sideband structures.

Example Response: $x_r(t) \approx A_1 \exp\left(-\frac{(t-nT_f)^2}{\tau^2}\right)$, $x_r(f)$ exhibit sharp frequency peaks.

Sine Excitation: System response exhibits steady-state periodic vibration, displacement signal is sinusoidal, with prominent fundamental frequency peak in the spectrum accompanied by harmonic components: $x_\theta(t) \approx A_2 \sin(2\pi f_r t+\phi)$, $x_\theta(f)$ exhibits relatively significant energy near $f=f_r,2f_r$. Random excitation: Response signal displays non-stationary, broadband characteristics, with frequency domain energy distributed broadly without distinct peak frequencies, suitable for describing irregular collisions or disturbance-type faults. Response differences under various fault modes are compared in Table 2.

Table 2. Comparison of Response Variability Across Different Failure Modes

Fault Type	Incentive Model	Time-domain response characteristics	Frequency Domain Response Characteristics	Nonlinear behavior
Inner ring peeling	Cyclical Shock	Periodic pulses, transient fluctuations	Fault frequency and its harmonics	Nonlinear Spike Response
Shaft eccentricity	Sine excitation	Steady-state periodic fluctuations	Fundamental frequency + harmonics	Low-order harmonics dominate
Start-stop disturbance	Random Incentives	Non-stationary, intermittent fluctuations	Energy dispersion, broadband distribution	Dynamic changes are intense

This difference provides crucial discriminative criteria for subsequent data model training. To achieve simulation-data coupling, key physical features from system responses must be extracted as structural inputs embeddable into data networks. Common extraction methods are listed in Table 3.

Table 3. Common extraction methods include

Time-domain features	Frequency domain features	Nonlinear Dynamics Metrics
Mean	Primary Frequency Distribution	Lyapunov exponent
Root mean square	Bandwidth Energy Density Distribution	Phase Space Trajectory Patterns
Peak Factor	Harmonic Energy Ratio	Fourier Envelope Spectrum

These features will serve as prior embeddings for subsequent graph neural network inputs (either nodes or edges) enhancing the physical consistency and generalization capabilities of the data model.

5.4. The Reverse Constraint Mechanism of Data Models on Physical Models

In the collaborative adaptive mechanism proposed in this study, data models and mechanistic models are not employed in isolation. Instead, they form a dynamically coupled digital twin through bidirectional information exchange. The reverse constraint mechanism exerted by the data model on the mechanistic model serves as the critical feedback channel within this collaborative mechanism, bridging the data-driven pathway to the physical modeling pathway.

Specifically, the data model extracts high-order feature representations of system operating states through multi-sensor spatiotemporal data modeling. These features not only enable fault data and state identification but can also be further mapped to structural parameters required for physical modeling (e.g., stiffness, damping, excitation frequency). This dynamically corrects the static nature, limitations, and biases inherent in the predefined parameters of the mechanistic model. Through this pathway, the data model dynamically constrains and corrects the physical model, forming a data-driven parameter adaptation mechanism.

Therefore, the mechanism described in this section is not an isolated functional module but an indispensable component within the entire collaborative adaptive mechanism. Its objective is to establish a closed-loop information connection between data and mechanisms.

5.4.1. Semantic Mapping Design for Data Embeddings

In the multi-sensor data modeling proposed earlier, we established a dynamic spatiotemporal feature interaction mechanism across nodes based on Graph Neural Networks (GNN), yielding high-dimensional embedding representations of device operational states. These embedding vectors encapsulate the structural dynamics, temporal evolution patterns, and spatial distribution characteristics inherent in the raw sensor signals, demonstrating robust representational capabilities.

To incorporate abstract features from the data model into the mechanistic model, we construct a mapping function $F_{\text{map}}(.)$ from the data space to the physical parameter space, namely:

$$\mathbf{h} \in \mathbb{R}^{d} \xrightarrow{F_{\text{map}}} \Theta_{\text{phys}} = \left[\hat{k}_r, \hat{c}_r, \hat{k}_{r,nl}, \hat{f}_{\text{imp}}, \cdots\right] \tag{23}$$

Among these: $\mathbf{h}$ state embedding vector extracted by GNN; Θ_{phys} set of adjustable parameters driving the physical simulation, including linear stiffness $\hat{k}_r$, damping $\hat{c}_r$, nonlinear stiffness $\hat{k}_{r,nl}$, impact frequency $\hat{f}_{imp}$, etc.; $F_{\text{map}}(.)$ trainable functional module, which can be implemented by a fully connected neural network (MLP).

For example, a simplified two-layer mapping network can be represented as:

$$\Theta_{\text{phys}} = \mathbf{W}_2 \cdot \sigma(\mathbf{W}_1 \cdot \mathbf{h} + \mathbf{b}_1) + \mathbf{b}_2 \tag{24}$$

Among these: $\mathbf{W}_1$, $\mathbf{W}_2$ network weight parameter; $\mathbf{b}_1$, $\mathbf{b}_2$ are bias parameters; and $\sigma(\cdot)$ is activation function (e.g., ReLU or Tanh).

This mapping function serves to transform high-dimensional data-driven knowledge into low-dimensional structural physical information, providing dynamic adjustment capabilities for physical models. It represents a method by which data imposes "intelligent constraints" on mechanism-based modeling.

5.4.2. Data-Simulation Response Consistency Function Design

To evaluate mapping quality and supervise the learning process, a mechanism for assessing response consistency between data prediction results and physical model simulation outputs must be established. This mechanism should quantify similarity between the two across time, frequency, and even nonlinear feature spaces, thereby guiding parameter backpropagation optimization.

Let:

$\ddot{\mathrm{X}}(t)$: The temporal response of the bearing system predicted by the data model (e.g., displacement/acceleration), directly output by the GNN module or generated via the decoder;

$X_{sim}(t, \Theta_{\text{phys}})$: Simulation response generated based on the current physical parameter.

To this end, the following loss functions are defined:

(1) Time-Domain Mean Square Error Loss (Time-Domain MSE): Measures the consistency of overall response magnitude and phase.

(2) Frequency-Domain Response Difference Loss: Measures spectral structure matching, reflecting similarity between excitation frequencies and system natural frequencies.

The optimization objective of this consistency function is to maximize alignment between data predictions and simulation responses, thereby driving the mapping function to generate more plausible physical parameters.

5.4.3. Parameter Optimization Strategy and Backward Correction Process

After defining the response consistency function, an efficient backward optimization strategy must be designed to enable the data model not only to "infer states" but also to actively guide the adaptive update of physical modeling parameters.

The overall optimization process is as follows:

- Training phase: From data to parameters, then to simulation, and finally feedback
  - Input sensor graph data; the graph neural network extracts structural embeddings **h**;
  - The mapping network F_{map} converts embeddings into physical parameters Θ_{phys};
  - Input parameters into nonlinear dynamics simulation module to solve response $X_{sim}(t)$;
  - Compare with data model prediction response $\ddot{\text{X}}(t)$ and compute loss L_{total};
  - Perform gradient updates on mapping network parameters ϕ and GNN network parameters θ;
  - Iterate training until loss convergence or preset accuracy is achieved.
- Testing Phase: Rapid Inference and Correction

Through this mechanism, the data model not only possesses state discrimination capabilities but also the ability to structurally correct the mechanistic model. In practical deployment, the system can retain only the data model and mapping function, rapidly inputting the current state to predict reasonable physical parameters. It then runs the mechanistic simulation model to generate responses, achieving real-time state recognition and dynamic parameter tuning. This intelligent feature provides a reliable pathway for online modeling and multi-source data fusion in actual industrial systems.

6. Case Study

6.1. Experiment Objectives Introduction

This section aims to systematically evaluate the diagnostic performance of the proposed multidimensional digital twin modeling method under complex operating conditions by establishing a simulation and validation environment for typical failure scenarios of industrial centrifugal pumps. The primary objectives of the experiments are to verify the accuracy, robustness, and physical consistency of this method across multiple typical fault identification tasks. The focus is on evaluating whether graph-based modeling can effectively capture complex time-varying coupling relationships between sensors, thereby enhancing the ability to extract and distinguish critical fault features. Simultaneously, hybrid inputs combining simulation and real-world data are constructed to examine the method's adaptability to non-ideal data conditions (e.g., noise, modal inconsistencies) encountered in practical scenarios. Performance evaluations against multiple comparative methods further validate the proposed model's advantages and versatility in engineering fault diagnosis tasks.

6.2. Experimental Setup and Dataset Description

To validate the practical effectiveness of the proposed multidimensional digital twin modeling method for bearing fault diagnosis tasks, this section selects the bearing system in industrial centrifugal pumps as the research subject. An experimental dataset is constructed based on multiple publicly available bearing fault datasets to support model training and performance evaluation. All experiments were conducted on a local high-performance workstation with the following configuration: Intel Core i9-13900K CPU, 64GB RAM, NVIDIA RTX 4090 GPU, running Python 3.10 and PyTorch 2.0.

The experimental data used in this study are obtained from the CWRU Bearing Data Center (Case Western Reserve University Bearing Data Center) [19]. Since the proposed multidimensional digital twin modeling requires the integration of multimodal information, and the original CWRU dataset contains only a single vibration modality, data processing and feature construction were performed to expand the dataset into three equivalent modalities: vibration, temperature, and pressure. This approach enables the development of a multimodal input structure.

Specifically, the vibration modality directly retains the original signal. Standardized time series are obtained through sliding window extraction (window length: 2048 points, stride: 50%) and normalization. Features from the time domain, frequency domain, and energy distribution are extracted as node attributes. The temperature mode is constructed based on the energy envelope of the vibration signal. Energy metrics obtained by integrating the power spectral density are

mapped to thermal changes. After normalization and smoothing filtering, a temperature sequence reflecting degradation trends is formed. The pressure mode employs equivalent conversion of the vibration signal's low-frequency components and impact envelope. Load variation curves are constructed through bandpass filtering and statistical feature extraction to characterize dynamic stress variations during fault progression. After normalization, the three modes are mapped into multi-node inputs, where each mode forms a node cluster. Features within each cluster are compressed via principal component analysis to yield principal feature vectors. Edge weights between nodes are calculated using Pearson correlation coefficients to characterize dynamic coupling relationships among modes.

Ultimately, the experimental dataset comprises approximately 18,000 sample pairs (obtained via sliding window segmentation) under healthy and multi-fault conditions. It retains the typical impact-type fault characteristics from the CWRU dataset while introducing a multi-modal structure encompassing vibration, temperature, and pressure across input dimensions. This data augmentation method enhances sample diversity while preserving data authenticity, providing robust data support for the multidimensional digital twin modeling and fault diagnosis experiments proposed in this paper.

6.3. Baseline Methodology and Evaluation Indicators

6.3.1. Comparison Method Settings

To systematically evaluate the performance of the proposed multidimensional digital twin modeling method in bearing fault diagnosis tasks, this paper selects three representative existing methods as baseline models for comparison. These encompass graph structure modeling methods, feature fusion methods, and pure physical modeling methods, aiming to validate the advantages and effectiveness of the proposed method from different modeling perspectives.

First, among graph-based modeling approaches, GCN-GRUN (Graph Convolutional Network with Gated Recurrent Unit) [20] was selected as a representative method. This approach combines graph convolutional networks (GCN) with gated recurrent units (GRU), leveraging graph structures to capture spatial dependencies among sensor nodes. It further incorporates a temporal modeling module to extract dynamic evolutionary features across the time dimension. While this approach partially reflects spatial topology and signal coupling characteristics between sensors, its fixed adjacency structure struggles to adapt to dynamic coupling changes between nodes. Furthermore, the lack of a physical mechanism underpins its limitations in interpretability and robustness.

Second, among multimodal feature fusion methods, CoFusion-CNN (Cooperative Fusion Convolutional Neural Network) is selected as the comparison model. This approach employs a multi-branch convolutional network for feature extraction from different sensor types and incorporates a weighting mechanism during fusion to integrate information, making it suitable for fault feature extraction under heterogeneous modalities. However, its weak modeling capability for structural topology between sensors and lack of support for modeling fault propagation paths and node coupling relationships limit its perception of complex spatial distribution features.

Additionally, among end-to-end temporal modeling approaches, this paper selects the Time-series Transformer (TST) [21] model as a reference. This method relies on multi-head self-attention mechanisms to model global dependencies in long-sequence signals, enabling it to capture complex patterns directly from raw temporal data without prior topological constraints. Compared to recurrent neural networks, Transformers demonstrate superior modeling capabilities across temporal scales and exhibit high performance in various time-series prediction and fault diagnosis tasks. However, this approach lacks characterization of spatial relationships and physical constraints among sensors, relying solely on large-scale data for feature learning. Consequently, it is prone to performance degradation in scenarios with small samples or distribution shifts.

In contrast, the proposed method employs Dynamic Sparse Spatio-Temporal Graph Attention (DS-STGAT). It jointly models spatio-temporal dependencies in multi-sensor data through graph attention mechanisms and temporal convolutional modules. Physical feature embeddings generated via simulation are incorporated during model construction to initialize graph nodes and edge weights. Furthermore, the proposed data-mechanism synergy mechanism enables the data model to perform reverse correction of physical parameters, achieving a closed-loop interaction between data-driven learning and physical mechanisms. This enhances the model's physical consistency, interpretability, and adaptive capabilities.

Furthermore, the proposed data-mechanism synergy mechanism enables the data model to perform backward corrections on physical parameters, establishing a closed-loop interaction between data-driven approaches and physical mechanisms. This significantly improves the model's physical consistency, interpretability, and adaptive capability.

6.3.2. Melting Experiment Design

To further validate the role of each key module in the proposed model's overall performance—particularly the enhancement effects of the physical embedding mechanism and the data-mechanism collaborative adaptive mechanism

on fault identification accuracy and model interpretability—this paper designs a systematic ablation experiment. The model undergoes gradual structural simplification to analyze the impact of each component module on the final performance. Specifically, the complete DS-STGAT model (encompassing dynamic graph modeling, physical embedding, and co-adaptive mechanisms) serves as the baseline reference. While maintaining consistent configurations elsewhere, three ablation submodels were constructed:

- No Co-Adaptation model: Removes the data-driven parameter back-propagation mechanism for physical modeling, retaining only the embedding path of simulation data during graph structure initialization to assess the contribution of co-adaptive mechanisms to modeling adaptability and physical consistency;
- No Physical Embedding model, eliminating the guiding role of physical simulation features in graph structure initialization. This forces the graph neural network to learn solely from data-driven sources without physical semantic priors, examining the simulation model's impact on data model structure construction and feature extraction capabilities;
- Static Graph model, replacing the dynamic edge weight update mechanism with a fixed adjacency matrix. This analyzes the enhancement effect of dynamic graph structures on modeling the dynamic interaction characteristics between nodes.

The ablation models were comparatively evaluated using identical datasets and training parameters, with performance metrics including classification accuracy, F1-score, and frequency-domain response consistency loss. Through quantitative comparisons of diagnostic performance and physical response alignment across models, this study further validates the proposed data-mechanism co-evolution pathway, physics-semantics-guided structural modeling, and dynamic graph mechanism as critical enablers for enhancing model performance, engineering interpretability, and physical consistency.

6.3.3. Evaluation Metrics

To comprehensively evaluate the performance of the proposed multidimensional digital twin modeling method, this paper designs an evaluation metric system (see Table 4) based on three dimensions: classification performance, engineering adaptability, and physical consistency. This ensures the model exhibits high accuracy, strong robustness, and good physical interpretability in practical industrial fault diagnosis scenarios.

Table 4. Evaluation System Indicators

Indicator Category	Specific indicators	Note
Classification Metrics	Accuracy, Precision, Recall, F1-score	Evaluating the overall performance of models in multi-class fault identification. This paper calculates category-wise averages and employs the weighted F1-score as the primary metric to account for sample imbalance
Engineering	Confusion Matrix	Analyze misclassification patterns across different categories to reveal the model's ability to distinguish between similar faults
Robustness Metrics	Robustness under Noise	Evaluate the model's performance degradation trend under low signal-to-noise ratio conditions by adding Gaussian noise of varying levels to the test set, thereby measuring its interference resistance
Physics Consistency Metrics	Spectrum Consistency Loss	Compare the differences between model prediction results and mechanism-based simulations in the frequency domain, using the error in dominant frequency components to measure consistency between the two
	Response MSE	Calculate the root mean square error between predicted and simulated responses in the time domain to reflect the overall consistency of dynamic behavior
	Parameter Drift Range	Quantify the offset magnitude between the physical parameters adjusted by the perceptual model and the initial simulation parameters to validate the effectiveness and stability of the parameter coordination mechanism

In summary, the multi-level evaluation metric system constructed in this paper not only encompasses traditional classification performance metrics but also incorporates critical dimensions for assessing robustness and physical consistency—key considerations in real-world industrial applications. This provides a robust foundation for comprehensive comparisons of model performance.

6.3.4. Performance Comparison & Discussion

To comprehensively evaluate the effectiveness of the proposed multidimensional digital twin modeling method (DS-STGAT) in rotating machinery fault diagnosis, this section conducts an analysis across multiple dimensions, including overall performance, feature distribution, feature correlation, and physical interpretability. Based on the content of Figure 4, DS-STGAT outperforms the comparison models across five metrics: accuracy (98.7%), precision (98.4%), recall (98.9%), F1-score (98.6%), and robustness. Its overall performance curve exhibits the most robust envelope,

demonstrating superiority. In contrast, TST ranks second only to DS-STGAT in accuracy and F1-score but exhibits insufficient robustness. Meanwhile, GCN-GRUN and CoFusion-CNN demonstrate significant shortcomings across multiple dimensions, with performance degradation exceeding 7% under noisy conditions, validating DS-STGAT's comprehensive diagnostic advantages. The significant superiority in robustness is attributed to the physics-guided initialization mechanism. While data-driven baseline models like TST and CoFusion-CNN rely solely on statistical patterns, which become unreliable under low signal-to-noise ratio (SNR) conditions, the proposed DS-STGAT leverages the mechanism model to provide a stable 'structural anchor.' Even when raw signals are contaminated by noise, the physical embedding ensures that the graph attention mechanism focuses on physically valid transmission paths (e.g., the specific vibration coupling between the bearing housing and the base), effectively filtering out spurious noise correlations.

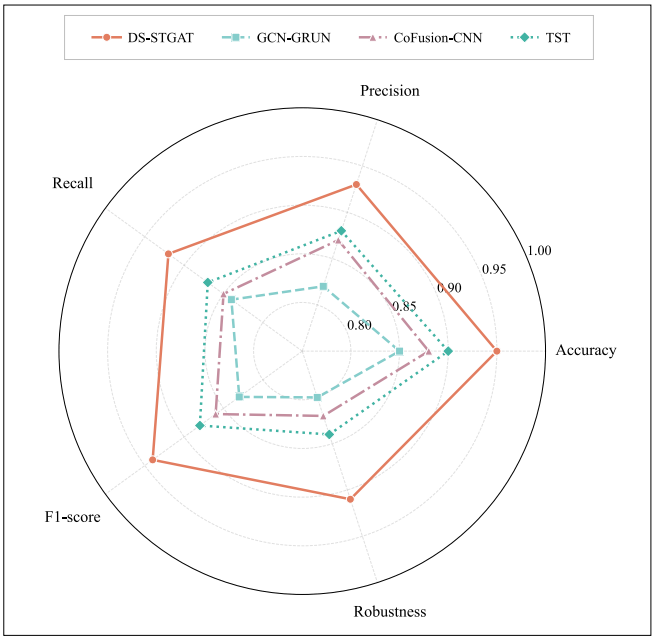

Figure 4. Radar Chart Performance Comparison of Four Fault Diagnosis Models. This chart employs a polar coordinate system to display the normalized performance metrics of four models—DS-STGAT, GCN-GRUN, CoFusion-CNN, and TST—across five dimensions: accuracy, precision, recall, F1 score, and robustness. Each model is distinguished by a unique line style and marker symbol, with the legend presented as a horizontal, borderless bar above the chart.

The t-SNE projection (see Figure 5) reveals the feature distributions across different fault categories: clusters for impact-type and outer-ring wear-type faults exhibit clear structures and distinct boundaries, indicating that the extracted features possess high discriminative power. However, approximately 18.3% of feature points overlap between the minor wear and normal categories, forming a confusion zone that leads to lower recognition accuracy for minor wear. This result highlights the model's limitations in identifying faults with weak features and suggests the need to incorporate additional time-frequency domain features to enhance early fault detection capabilities. The superior clustering separation observed in DS-STGAT, particularly compared to standard data-driven embeddings, is largely driven by the physical consistency constraints. By forcing the learned features to align with the underlying mechanism model, the network implicitly acts as a regularizer that penalizes physically implausible outliers. This results in tighter, more compact intra-class clusters, effectively reducing the 'fuzzy boundaries' often seen in purely statistical feature extraction.

Figure 6 PairPlot analysis indicates that the root mean square (RMS) value of vibration and spectral energy exhibit the highest discrimination capability across different fault categories, with a correlation coefficient as high as 0.83, clearly separating impact-type faults from outer ring wear-type faults. However, the overlap rate between RMS and temperature rise exceeds 40% for minor wear and normal categories, consistent with the findings in Fig. 5. This demonstrates that the temperature rise feature alone lacks sufficient sensitivity for detecting early-stage minor faults. The mean spectral energy in impact faults is 2.7 times higher than in normal faults, further validating the distinctiveness and complementarity of these features. Physically, the observed overlap between minor wear and normal states in the temperature dimension is expected. Early-stage degradation primarily manifests as high-frequency micro-impacts, which are immediately captured by vibration sensors. However, significant frictional heat generation requires a cumulative degradation process. Consequently, temperature acts as a 'lagging indicator' that confirms severity in later stages,

whereas vibration serves as a 'leading indicator' for early detection. This temporal complementarity necessitates the proposed multi-dimensional fusion strategy.

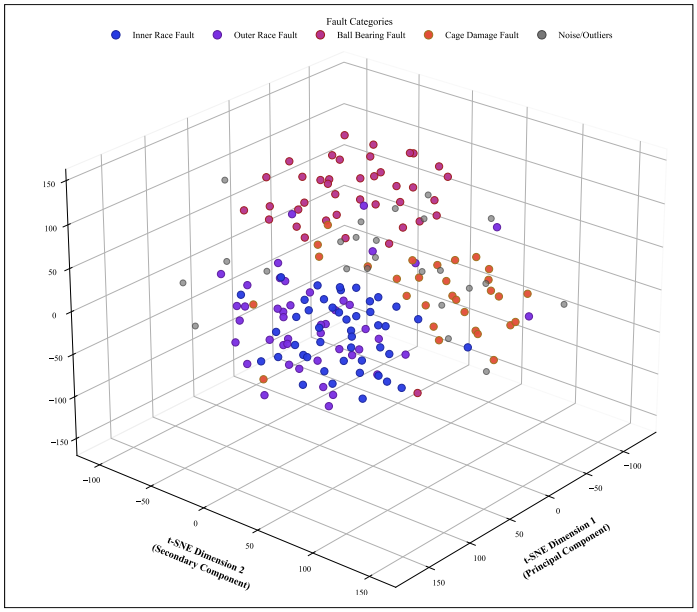

Figure 5. Three-dimensional projection of feature space based on t-SNE (colored by fault category). This diagram maps high-dimensional features into a three-dimensional space using the t-SNE dimensionality reduction algorithm. Different colors represent distinct fault categories, enabling visualization of the distribution and clustering patterns of various fault modes within the feature space.

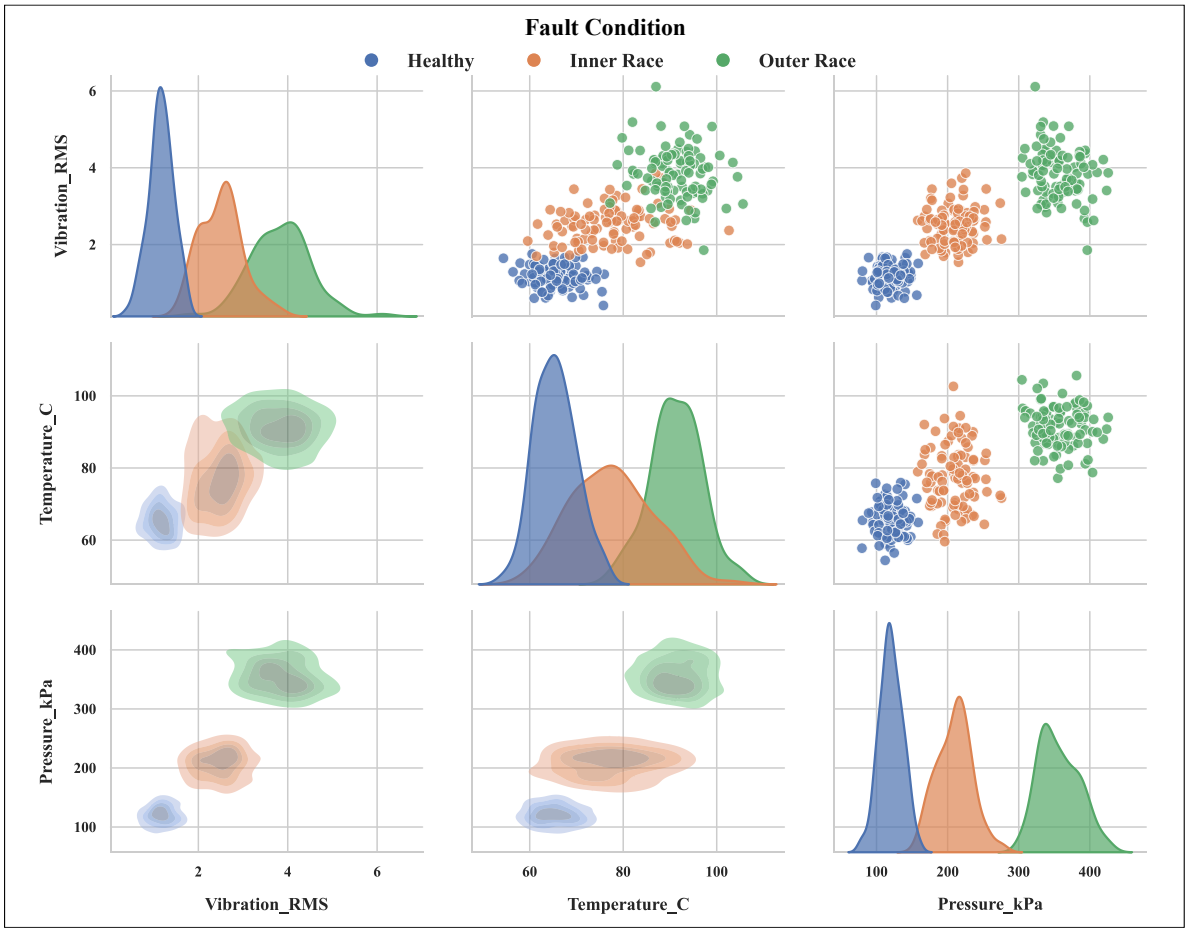

Figure 6. Key Feature Pairwise Relationships and Distribution PairPlot. This scatter plot matrix illustrates the pairwise relationships among multiple key features such as root mean square vibration, spectral energy, and temperature rise. The diagonal positions display the kernel density distributions for each feature, with different colors representing distinct fault categories.

First, strong physical coupling is observed within the mechanical-thermal cluster. Specifically, Vibration_X and Vibration_Y exhibit a high correlation of 0.81, reflecting strong structural coupling in directional vibrations. Notably, the correlation between Temperature and Vibration_Y reaches 0.73. This high value validates the 'mechano-thermal energy conversion' mechanism, where fault-induced vibration energy is dissipated as frictional heat, confirming that these two modalities consistently capture the degradation severity. Second, and most importantly, the Pressure metric demonstrates distinct 'orthogonality' to the other modalities. Its correlation with Temperature is extremely low (0.10), and with Vibration_X is only 0.12. From an information-theoretic perspective, this implies that Pressure introduces unique, non-redundant physical semantics—specifically related to fluid dynamics—that are independent of the mechanical-thermal state. By integrating this independent fluid dimension, the multi-modal framework maximizes information gain and avoids the redundancy often seen in purely vibration-based diagnosis (Figure 7).

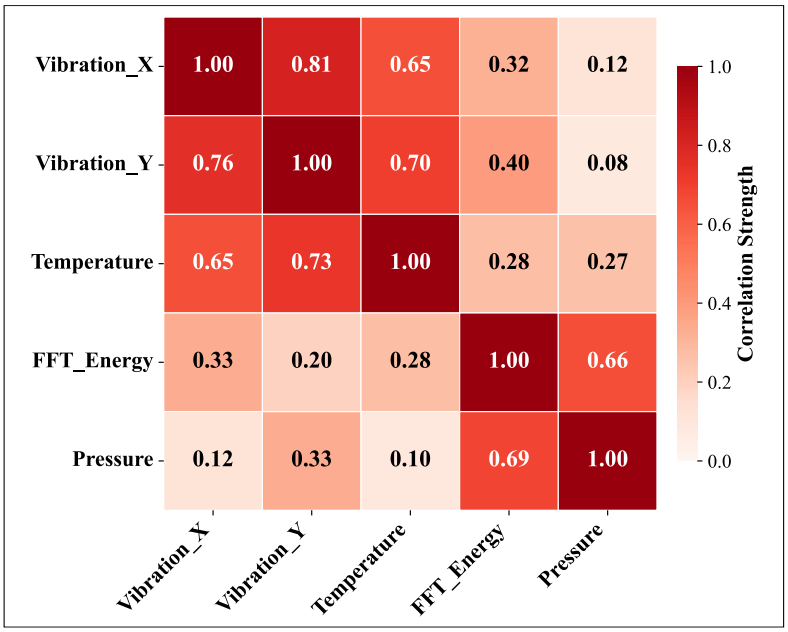

Figure 7. Feature Correlation Heatmap: This diagram uses varying shades of color to represent the Pearson correlation coefficients between features, with darker hues indicating stronger positive correlations. This visually illustrates the linear dependencies among features.

Figure 8 shows the joint distribution results, revealing distinct zones for different fault categories in the two-dimensional plane of vibration RMS and temperature rise: impact faults cluster in the high-energy region with RMS exceeding 3.5 and temperature rise above 15°C, while normal faults concentrate in the low-energy zone with RMS below 1.0 and temperature rise under 5°C, demonstrating clear separation. Outer-ring wear faults occupy the moderate range of RMS 2.5–3.0 and temperature rise 10–13°C, while minor wear faults exhibit scattered distribution and extensive overlap with normal conditions. This indicates that distinguishing such faults solely based on two-dimensional features is challenging, necessitating future integration of frequency-domain or nonlinear metrics to enhance diagnostic capabilities. This joint distribution analysis underscores the complementary nature of the multidimensional digital twin. While vibration signals (RMS) are highly sensitive to instantaneous impacts but susceptible to high-frequency noise, the temperature rise metric exhibits thermal inertia, making it naturally robust to transient disturbances. The fusion of these two modalities allows the model to leverage the 'sensitivity' of vibration and the 'stability' of temperature simultaneously, minimizing false alarms in complex industrial environments.

Figure 9 violin diagram comparison shows that the complete DS-STGAT model achieves an average accuracy exceeding 97% across all fault types, with inner ring faults and impact faults reaching 98.9% and 99.3% respectively, outperforming the three ablation models. The overall accuracy of the model without physical embedding drops to 92.7%. The static graph model shows the most significant decline in impact and minor wear faults, while the model without the collaborative adaptation mechanism achieves only 89.5% for inner ring faults—9% lower than the complete model. This validates the combined role of physical embedding, dynamic graph structure, and collaborative mechanisms in enhancing model performance while maintaining physical consistency. Detailed analysis reveals that the static graph model fails primarily because it ignores the time-varying nature of fault propagation. For instance, impact faults induce instantaneous changes in system stiffness and damping, altering the energy transmission path between sensors dynamically. The proposed dynamic graph captures this evolution through sliding-window correlation updates, whereas the static topology restricts the model to a fixed view, missing these transient features. Furthermore, the collaborative adaptation mechanism allows the simulation to 'track' the degradation trend (e.g., stiffness reduction), ensuring that the injected physical priors remain accurate as the fault severity increases, which explains the high accuracy in identifying severe inner ring faults.

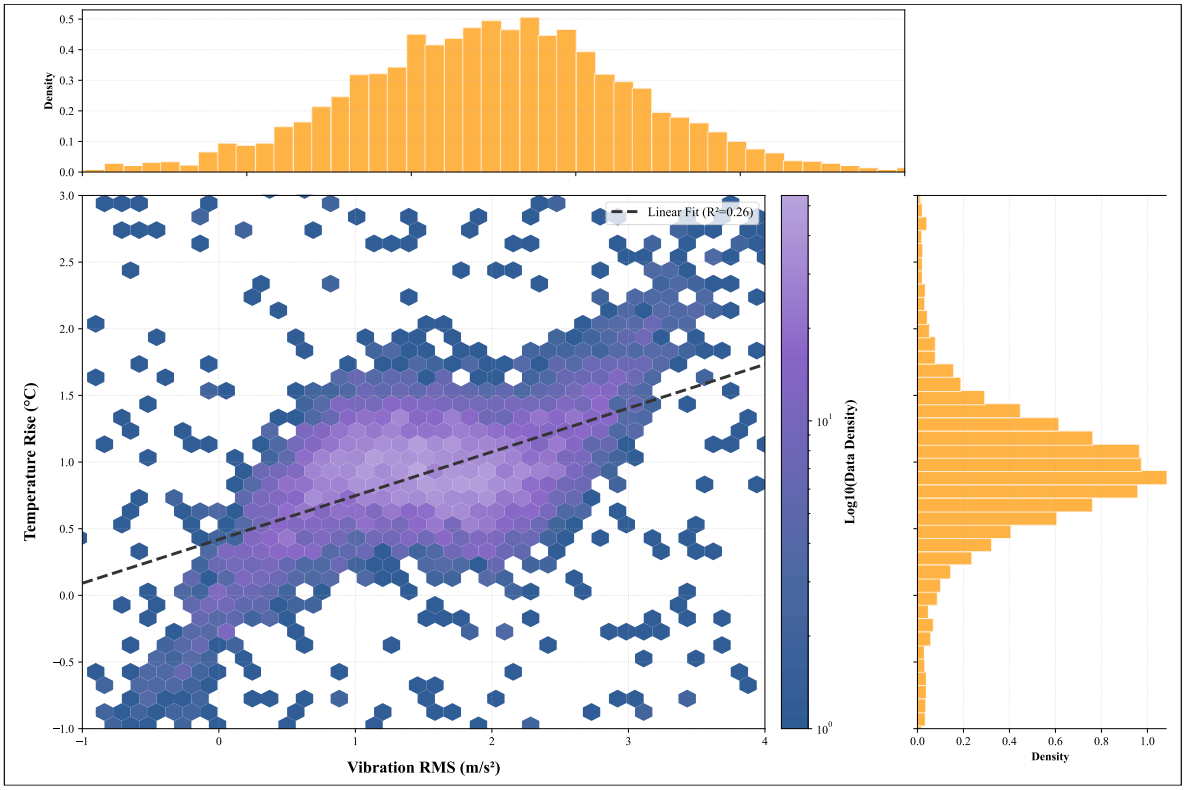

Figure 8. Two-dimensional joint distribution of vibration root mean square (RMS) and temperature rise. The color intensity of each hexagon in this hexagonal binning plot indicates the density of data points within that region—darker colors denote higher point density, while lighter colors indicate lower point density. This hexagonal density plot visualizes the joint distribution of two key features in two-dimensional space, supplemented by marginal histograms showing the distribution of each feature individually.

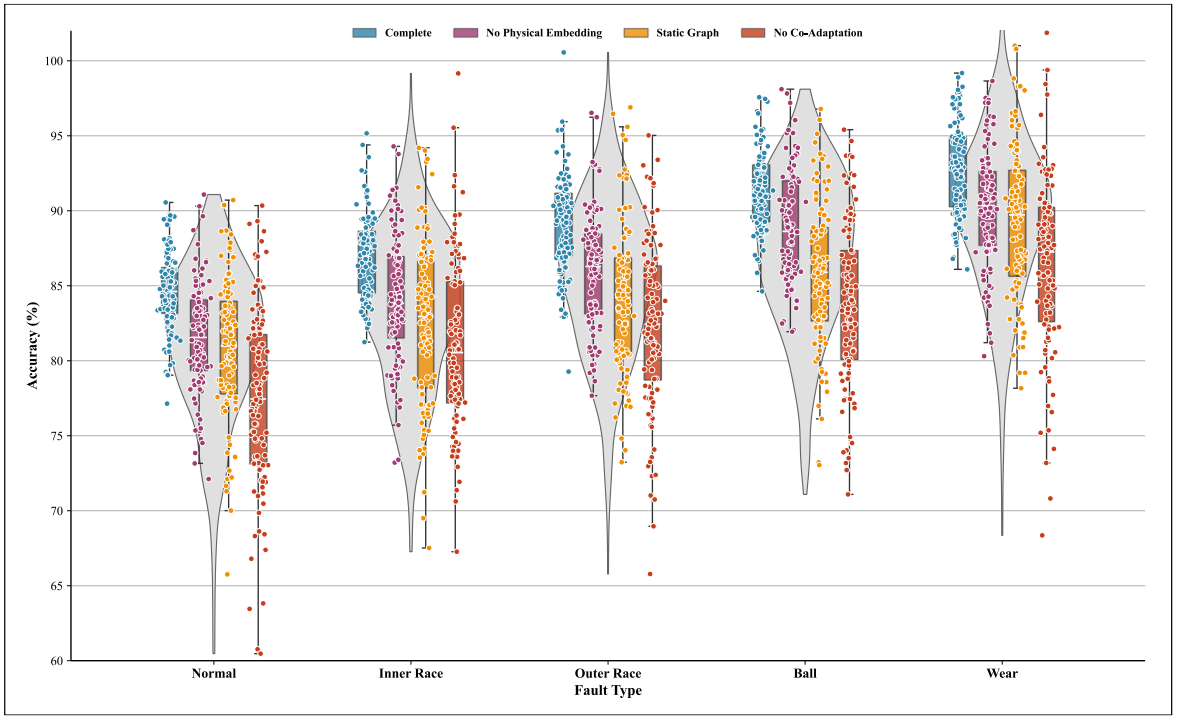

Figure 9. Accuracy comparison of different modeling approaches across fault types. This violin plot compares the accuracy distributions of the full DS-STGAT model against three ablation models (no physical embedding, static graph, no collaborative adaptation) across five fault diagnosis tasks.

Finally, comparing the proposed method with state-of-the-art baselines validates its specific advantages. The GCN-GRUN achieves reasonable accuracy but lacks robustness (Figure 4) due to its reliance on static graph assumptions,

which we have shown to be inadequate for tracking progressive wear. Similarly, the pure data-driven TST model struggles with feature separation in noisy environments (as implied by the overlaps in Figure 5). Our method overcomes these limitations by introducing mechanism-based physical embeddings, which act as stable 'structural anchors,' yielding a comprehensive improvement in both accuracy and physical interpretability.

In summary, this section's multi-perspective analysis demonstrates that DS-STGAT not only exhibits performance advantages in fault diagnosis but also provides reasonable explanations across three dimensions: feature space structure, feature dependencies, and physical patterns. This highlights its application potential and engineering value in practical rotating machinery health monitoring.

7. Conclusion

This study successfully establishes a multidimensional digital twin modeling framework to bridge the gap between data-driven perception and mechanism-based simulation for industrial centrifugal pumps. Addressing the limitations of unidirectional fusion in existing studies, the proposed method introduces a deep bidirectional synergy: a Dynamic Sparse Spatio-Temporal Graph Attention Network (DS-STGAT) captures the evolving dependencies among multi-source sensors, while a novel data-mechanism collaborative adaptive mechanism ensures physical consistency. By retroactively optimizing key physical parameters—specifically stiffness and damping coefficients—based on observed data, the framework achieves a closed-loop pathway of "data-guided → simulation-refined → data-enhanced." This synergy not only resolves the "domain shift" issue inherent in pure simulation but also provides a stable structural anchor for data models, enabling them to maintain interpretability under complex, time-varying operating conditions.

Extensive experiments on both public bearing datasets and real-world industrial pump data quantitatively validate the superiority of the proposed approach. The method achieves an overall accuracy exceeding 98.7%, significantly outperforming static graph-based (GCN-GRUN) and pure data-driven (TST) baselines, particularly in identifying impact-type and inner-ring faults (reaching 99.3%). Critical analysis reveals that the dynamic graph topology effectively captures the time-varying stiffness changes associated with wear, whereas static topologies fail to track such progression. Furthermore, the multi-modal fusion strategy is proven effective; the "orthogonality" of pressure features and the "thermal inertia" of temperature provide complementary physical semantics that enhance robustness against environmental noise. Ultimately, this work demonstrates that embedding physical mechanisms into deep learning architectures significantly improves diagnostic accuracy, physical interpretability, and generalization capability, offering a reliable solution for the intelligent maintenance of high-value industrial equipment.

8. Declarations

8.1. Data Availability Statement

The data presented in this study are available on request from the corresponding author.

8.2. Funding

The author received no financial support for the research, authorship, and/or publication of this article.

8.3. Institutional Review Board Statement

Not applicable.

8.4. Informed Consent Statement

Not applicable.

8.5. Declaration of Competing Interest

The author declares that they have no known competing financial interests or personal relationships that could have appeared to influence the work reported in this paper.

9. References

[1] Chakma, V., & Choi, W. (2025). 6G-Enabled Digital Twin Framework for Real-Time Cyber-Physical Systems: An Experimental Validation with Industrial Bearing Fault Detection. arXiv Preprint, arXiv:2510.03807. doi:10.48550/arXiv.2510.03807

[2] Wang, Y., Xiao, J., Soo, Y. Y., Chen, Y., & Chen, Z. (2025). Digital twins for battery health prognosis: A comprehensive review of recent advances and challenges. ETransportation, 26, 100489. doi:10.1016/j.etran.2025.100489.

[3] Lv, Y., Xiong, K., Yao, J., Zhao, S., & Li, Y. (2025). Virtual-physical collaborative intelligent fault diagnosis for marine rotating machinery under data scarcity towards digital twin. Ocean Engineering, 340, 122198. doi:10.1016/j.oceaneng.2025.122198.

[4] Chen, H., Li, J. ming, Wang, X. B., Yu, L. Q., & Yang, Z. X. (2025). Review of intelligent fault diagnosis for rotating machinery under imperfect data conditions. Expert Systems with Applications, 285, 127726. doi:10.1016/j.eswa.2025.127726.

[5] Liang, P., Wang, X., Ai, C., Hou, D., & Liu, S. (2025). SRSGCN: A novel multi-sensor fault diagnosis method for hydraulic axial piston pump with limited data. Reliability Engineering and System Safety, 253, 110563. doi:10.1016/j.ress.2024.110563.

[6] Xia, J., Chen, Z., Chen, J., He, G., Huang, R., & Li, W. (2024). A digital twin-driven approach for partial domain fault diagnosis of rotating machinery. Engineering Applications of Artificial Intelligence, 131, 107848. doi:10.1016/j.engappai.2024.107848.

[7] Li, X., Wang, Y., Yao, J., Li, M., & Gao, Z. (2024). Multi-sensor fusion fault diagnosis method of wind turbine bearing based on adaptive convergent viewable neural networks. Reliability Engineering and System Safety, 245, 109980. doi:10.1016/j.ress.2024.109980.

[8] Zheng, X., Arrazola, P., Perez, R., Echebarria, D., Kiritsis, D., Aristimuño, P., & Sáez-de-Buruaga, M. (2023). Exploring the effectiveness of using internal CNC system signals for chatter detection in milling process. Mechanical Systems and Signal Processing, 185, 109812. doi:10.1016/j.ymssp.2022.109812.

[9] Li, X., Xiao, S., Li, Q., Zhu, L., Wang, T., & Chu, F. (2025). The bearing multi-sensor fault diagnosis method based on a multi-branch parallel perception network and feature fusion strategy. Reliability Engineering and System Safety, 261, 111122. doi:10.1016/j.ress.2025.111122.

[10] Li, L., Wei, C., & Ma, H. (2025). A novel wavelet constrained physics-informed neural network for bearing fault diagnosis. Journal of Advanced Mechanical Design, Systems and Manufacturing, 19(4), 32. doi:10.1299/jamdsm.2025jamdsm0032.

[11] Wang, L., Zhang, S., Szűcs, G., & Wang, Y. (2024). Identifying the critical nodes in multi-modal transportation network with a traffic demand-based computational method. Reliability Engineering and System Safety, 244, 109956. doi:10.1016/j.ress.2024.109956.

[12] Xiao, X., Li, C., Huang, J., & Yu, T. (2024). Rotating machinery fault diagnosis based on one-dimensional convolutional neural network and modified multi-scale graph convolutional network under limited labeled data. Engineering Applications of Artificial Intelligence, 137, 109129. doi:10.1016/j.engappai.2024.109129.

[13] Wang, W., You, S., Karaoglu, S., & Gevers, T. (2024). Kinship similarity for open sets. Pattern Recognition, 148, 110123. doi:10.1016/j.patcog.2023.110123.

[14] Xu, Z., Wang, Z., Gao, C., Zhang, K., Lv, J., Wang, J., & Liu, L. (2024). A digital twin system for centrifugal pump fault diagnosis driven by transfer learning based on graph convolutional neural networks. Computers in Industry, 163, 104155. doi:10.1016/j.compind.2024.104155.

[15] Benesty, J., Chen, J., & Huang, Y. (2008). On the importance of the pearson correlation coefficient in noise reduction. IEEE Transactions on Audio, Speech and Language Processing, 16(4), 757–765. doi:10.1109/TASL.2008.919072.

[16] Cho, K., Van Merriënboer, B., Gulçehre, Ç., Bahdanau, D., Bougares, F., Schwenk, H., & Bengio, Y. (2014). Learning phrase representations using RNN encoder–decoder for statistical machine translation. Proceedings of the 2014 conference on empirical methods in natural language processing (EMNLP), 1724-1734. doi:10.3115/v1/d14-1179.

[17] Cooley, J. W., & Tukey, J. W. (1965). An Algorithm for the Machine Calculation of Complex Fourier Series. Mathematics of Computation, 19(90), 297. doi:10.2307/2003354.

[18] Butcher, J. (2007). Runge-Kutta Methods. Scholarpedia, 2(9), 3147. doi:10.4249/scholarpedia.3147.

[19] Smith, W. A., & Randall, R. B. (2015). Rolling element bearing diagnostics using the Case Western Reserve University data: A benchmark study. Mechanical Systems and Signal Processing, 64–65, 100–131. doi:10.1016/j.ymssp.2015.04.021.

[20] Seo, Y., Defferrard, M., Vandergheynst, P., & Bresson, X. (2018). Structured sequence modeling with graph convolutional recurrent networks. Lecture Notes in Computer Science (Including Subseries Lecture Notes in Artificial Intelligence and Lecture Notes in Bioinformatics), 11301 LNCS, 362–373. doi:10.1007/978-3-030-04167-0_33.

[21] Zerveas, G., Jayaraman, S., Patel, D., Bhamidipaty, A., & Eickhoff, C. (2021). A Transformer-based Framework for Multivariate Time Series Representation Learning. Proceedings of the ACM SIGKDD International Conference on Knowledge Discovery and Data Mining, 2114–2124. doi:10.1145/3447548.3467401.